RNA interference microarrays: High-throughput loss-of-function genetics in mammalian cells

Jose M. Silva, Hana Mizuno, Amy Brady, Robert Lucito, and Gregory J. Hannon*

Watson School of Biological Sciences, Cold Spring Harbor Laboratory, 1 Bungtown Road, Cold Spring Harbor, NY 11724

RNA interference (RNAi) is a biological process in which a double-stranded RNA directs the silencing of target genes in a sequence-specific manner. Exogenously delivered or endogenously encoded double-stranded RNAs can enter the RNAi pathway and guide the suppression of transgenes and cellular genes. This technique has emerged as a powerful tool for reverse genetic studies aimed toward the elucidation of gene function in numerous biological models. Two approaches, the use of small interfering RNAs and short hairpin RNAs (shRNAs), have been developed to permit the application of RNAi technology in mammalian cells. Here we describe the use of a shRNA-based live-cell microarray that allows simple, low-cost, high-throughput screening of phenotypes caused by the silencing of specific endogenous genes. This approach is a variation of "reverse transfection" in which mammalian cells are cultured on a microarray slide spotted with different shRNAs in a transfection carrier. Individual cell clusters become transfected with a defined shRNA that directs the inhibition of a particular gene of interest, potentially producing a specific phenotype. We have validated this approach by targeting genes involved in cytokinesis and proteasome-mediated proteolysis.

RNA interference (RNAi) has emerged as one of the standard techniques to study gene function in diverse experimental systems. Introduction of double-stranded RNA (dsRNA) into a cell decreases the level of the complementary mRNAs producing a knockdown of the corresponding protein. The current model of the RNAi mechanism proposes that the silencing "trigger" is processed by Dicer into small RNAs of 21–22 nucleotides in length. These become incorporated into an RNA-induced silencing complex with endonuclease activity (RISC), which, in turn, identifies and cleaves homologous mRNAs (1, 2).

Based on this approach, genomewide RNAi approaches have been used successfully for phenotype-based screens in *Caenorhabditis elegans* (3–5) and *Drosophila melanogaster* (6, 7). In part, these successes derive from the availability of convenient and inexpensive methods for producing and introducing dsRNA. For example, it has previously been shown that RNAi can be triggered by soaking *C. elegans* in a solution of dsRNA (8), or by feeding worms with *E. coli* expressing gene-specific dsRNAs (9). In *Drosophila* cells a soaking protocol is also available allowing an easy method of introducing dsRNA (10).

Unfortunately, similarly straightforward approaches for triggering silencing have not been described in mammals. Analysis of multiples genes requires a "gene by gene" method, in which individual transfections must be performed, making these studies expensive, tedious, and dependent on high-throughput robotic systems. Cell microarrays represent a novel alternative to classical approaches to phenotype-based assays in mammalian cells.

Cell microarrays were first described by Ziauddin and Sabatini (11), who demonstrated that cells grown on a glass substrate could take up DNA–lipid complexes that had been deposited on the slide before cells were plated. Cells essentially became transfected *in situ*, with defined spots of transfected cells localized over the printed DNAs. These studies demonstrated the use of conventional DNA constructs for creating phenotypes based on ectopic expression. Here we investigate the possibility of

similarly using cell microarrays for loss-of-function genetics. This is accomplished by creating a microarray of living cells that have been transfected *in situ* with either small interfering RNAs (siRNAs) or with DNA constructs that direct the expression of short hairpin RNAs (shRNAs). These are effective at initiating a silencing response and in creating defined areas (spots) of cells in which suppression of a targeted gene generates an expected phenotype. Such arrays will find broad application to high-throughput low-cost phenotype-based screens in mammalian cells.

Materials and Methods

Microarray Printing and Reverse Transfection. Transfection mixes containing DNA reporter vectors (500 ng) plus shRNAs (1 μg) or siRNAs (200 ng) were printed onto glass slides by using a previously described "lipid method" (11) with some modifications. Briefly, nucleic acids were resuspended in 15 μl of DNA-condensation buffer (Buffer EC, Qiagen, Valencia, CA) with a final concentration of 0.4 M sucrose. After two incubation steps with the enhancer solution and the Effectene transfection reagent (Qiagen), a 1× volume of 0.2% gelatin was remixed with the solution to complete a transfection master mix of 45 μl. Ten microliters of this was aliquotted into a 384-well plate for printing, and the remaining 35 μl was stored at 4°C for later assays. Samples were printed onto Corning GAPS II slides with a PixSys 5500 Robotic Arrayer (Genomic Solutions, Ann Arbor, MI). Pins transferred the "lipid–DNA" solution to the slide while touching the surface of the slide for 500 ns. To ensure enough printed area to contain several hundred cells, we printed in close proximity nine spots forming a 3 × 3 square. After printing, the nine spots fuse together forming a bigger single dot with a diameter of ≈400–500 μm. To prevent contamination after printing, the slides were dried overnight at room temperature in a tissue culture hood.

To perform the reverse transfection, one spotted array was placed inside a 10-cm tissue culture dish and 15 ml of media containing cells at a concentration of 1×10^6 per milliliter was added into the dish taking care not to disturb the printed surface. Cells were incubated for 60 h without media change before analysis of the results (Fig. 1).

Reporter Assays. One hundred sixty dots containing a dual reporter vector expressing GFP/dsRed fluorescent proteins (gift of Alla Karpova, Cold Spring Harbor Laboratory) and individual shRNAs were printed. All shRNA were part of a library of U6 polymerase III promoter-driven hairpins (28). Four groups of experiments with 40 dots (each) were printed: the first group contained only dual reporter vector, the second group contained the reporter vector plus an shRNA or siRNA against firefly luciferase (Ff shRNA and Ff siRNA), the third group contained
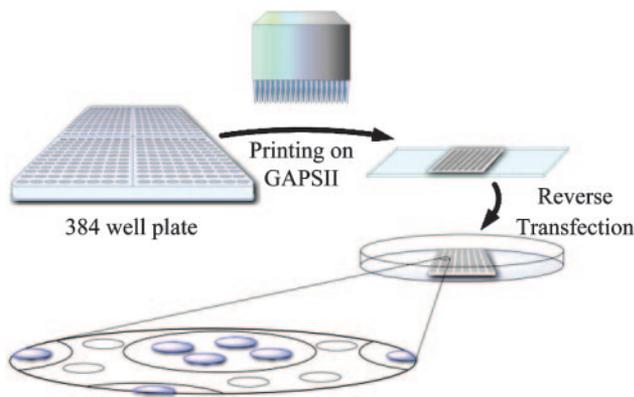

Fig. 1. Outline of the protocol used to perform reverse transfection on a glass slide. Transfection mixes containing gelatin were spotted on GAPS II glass slides with a PixSys 5500 Robotic Arrayer to form a 3 × 3 square. Dried slides were put inside a 10-cm tissue culture dish, and medium with cells was added to the dish. After incubation, groups of transfected cells could be detected inside the spotted transfection mixes.

the reporter vector plus a shRNA or a siRNA against GFP that has no effect in the expression level of the protein (GFP shRNA-1 and GFP siRNA-1), and the last group contained the reporter vector plus a shRNA that reduces by 90% the GFP signal when tested in culture plates (GFP shRNA-2 and GFP siRNA-2).

Several cell lines were tested for transfection, NIH 3T3, IMR90/E1A, HeLa, and HEK 293T. To test the stability of the printed array, we repeated the assay at different time points after printing, day 0, 1 week, 2 weeks, 4 weeks, and 2 months. For testing the stability of the transfection master mix, we stored the solution at 4°C and then printed new slides and assayed them at the time points described above.

Proteasome-Mediated Proteolysis Assays. Thirty shRNAs targeting different proteasome subunits were printed in triplicate. Every dot harbored an shRNA-expression vector, a plasmid expressing dsRed (dsRed N-1, Clontech), and a vector encoding a proteasome fluorescent reporter (ZsProSensor, Clontech). This reporter encodes a fusion protein that has been engineered to show varying levels of expression depending on the status of the proteasome pathway. Every transfection master mix contained 400 ng of dsRed vector, 100 ng of ZsProSensor, and 1 μg of shRNA plasmid. Twenty micrograms of total protein lysates was used for Western blot analysis. Rabbit anti-PSMC-6 subunit of the proteasome (Affinity, Biomol, Plymouth Meeting, PA), rabbit anti-ubiquitin (StressGen Biotechnologies, Victoria, Canada), and mouse anti-β-actin (United States Biological, Swampscott, MA) antibodies were also used in these studies.

Cytokinesis Defect Assays. Eight shRNAs targeting the motor protein Eg5 were printed (10 replicas each) together with a vector encoding an α-tubulin-GFP fusion protein (GFP-tubulin, Clontech). Every transfection mix contained 1 μg of Eg5 hairpin and 500 ng of the fluorescent fusion protein expression plasmids.

For immunofluorescence studies, we printed a replica slide where the transfection mix contained 500 ng of the dsRed reporter instead of the GFP-tubulin. Cells were stained by using standard methods with small variations. After incubation of the slides for 60 h the cells were fixed with paraformaldehyde for 10 min, washed very gently, and permeabilized with 1% Triton X-100 in PBS for 15 min on ice. Only one 15-min wash was performed to avoid washing away the cells. Mouse anti-α-tubulin (Sigma) was used in this study. Hoechst dye was included in the last wash to visualize the chromosomes.

Ninety-Six-Well Plate Analyses. All RNAi microarray results were validated by using cells transfected in 96-well tissue culture plates. Cells were transfected with LT-1 (Mirus, Madison, WI) according to the manufacturer's instructions at 50–70% confluence. The plasmids containing appropriate constructs were cotransfected, keeping the same ratios used in the arrayed slides but with a total mass of 100 ng of DNA for each transfected well. Again, results were analyzed after 60 h of incubation.

Results

Targeting Reporter Genes *in Situ* by Using siRNAs. Given previous successes in ectopically expressing genes by reverse transfection (11), we hoped that similar approaches could be coupled with the use of RNAi to produce knockdown phenotypes. Therefore, we began by testing the ability of siRNAs to be deposited on a microarray as lipid–RNA complexes and to cause sequence-specific silencing in cells grown on the arrays. We began by testing the ability of siRNAs to silence a co-delivered, ectopic marker. For convenience, we used GFP to enable both transfection and silencing to be scored by visual inspection. Because GFP was the siRNA target, we also included a plasmid that directs the expression of a second fluorescent protein (dsRed) to allow us to verify that siRNAs specifically silenced GFP expression rather than simply interfered with transfection.

Several siRNAs homologous to the GFP coding sequence were mixed with plasmids encoding GFP and dsRed. Nucleic acids were combined with a variety of lipid reagents [LT-1 or TKO (Mirus) and Effectene (Qiagen)], and the lipid–nucleic acid complexes were spotted onto glass slides. We found that Qiagen reagent performed best, giving optimal transfection of both DNA and RNA in this experiment. GFP siRNAs that had been previously identified as an efficient suppressor of the expression of the fluorescent protein in standard transfections (GFP siRNA-2) also showed potency on the spotted array. Ineffective siRNAs (GFP siRNA-1) or unrelated siRNAs (Ff siRNA) did not produce any effect on GFP expression levels either in standard transfections or on microarray slides (Fig. 2*A*).

Targeting Reporter Genes *in Situ* by Using shRNAs. The aforementioned studies demonstrated that an RNAi response could be initiated by *in situ* transfection of siRNAs on glass-slide microarrays. As stated above, RNAi can also be initiated in mammalian cells by transfection of DNA expression constructs that direct the synthesis of shRNA sequences. We therefore tested the possibility that a slide printed with a transfection mix containing an shRNA-expression construct that targets a specific mRNA could initiate a specific silencing response in *in situ* transfected cell clusters. As a first step, we again tested our ability to down-regulate the expression of GFP. Spots were printed as described above. In every cell cluster, the GFP level reported specific RNAi-mediated suppression and the dsRed level again acted as a transfection control.

As expected, none of the spots containing the reporter vector alone, the reporter plus a control shRNA, targeting firefly luciferase, or the reporter plus GFP shRNA-1, an ineffective shRNA, showed any reduction in the expression of GFP. In contrast, all spots harboring the GFP shRNA-2, an active shRNA, presented a strong attenuation of the GFP signal while maintaining unaltered levels of dsRed protein (Fig. 2*B*). It is worth noting that all suppressed samples showed a similar degree of attenuation of GFP and a very similar percentage of transfected cells, revealing a high degree of consistency from spot to spot.

We next asked whether the *in situ* RNAi procedure could be applied broadly by examining the response of a number of different cell lines in an arrayed format. These included transformed and nontransformed cells lines, fibroblasts and epithelial cells, and lines from mouse and human. Of those tested, HEK
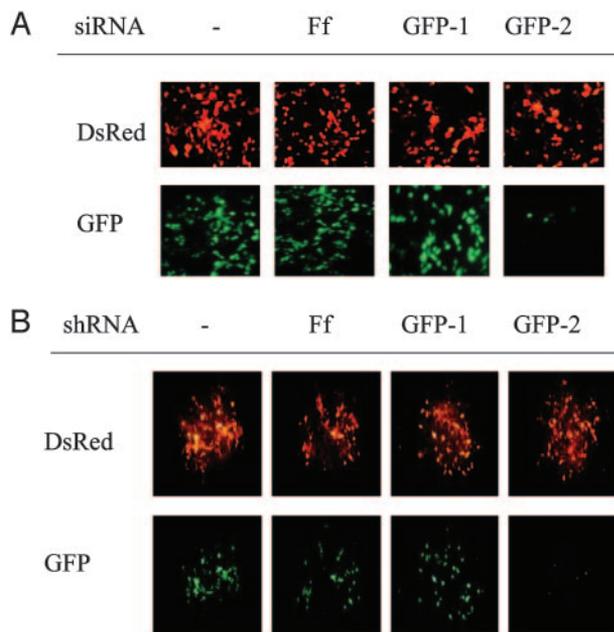
GENETICS

Fig. 2. The GFP reporter is specifically suppressed by RNAi in 293T cells incubated for 48 h on a printed glass slide. (*A*) Printed spots contained a vector expressing GFP and dsRed reporters and individual siRNAs targeting different sequences (as indicated): no siRNA (—), Ff, siRNA-1 (GFP-1), and siRNA-2 (GFP-2). (*B*) Printed spots contained a vector expressing GFP and dsRed reporters and individual shRNA expression plasmids targeting different sequences (as indicated): no hairpin (-), Ff, hairpin 1 (GFP-1), and hairpin 2 (GFP-2). Control spots harbored siRNA or an shRNA-expression vector against Ff, GFP-1, or no added RNAi inducer (mock).

Fig. 3. (*A*) Different levels of ZsGreen protein accumulation detected in the RNAi microarray. (*B*) HEK 293T were incubated with individual hairpins targeting the expression of different proteasome subunits. A Western blot shows specific inhibition of ATPase-6 shRNA. Firefly shRNA was used as control. (*C*) Anti-ubiquitin Western blot showing accumulation of polyubiquitinated proteins in treated cells.

293T cells showed the highest efficiency. IMR90/E1A, NIH 3T3, and HeLa cells showed lower efficiency (20–50%) than 293T (data not shown). Our results indicate that by varying the lipid and nucleic acid content of the spot, many different cell lines can be used. However, for convenience, we performed the remainder of our assays with HEK 293T.

We also examined the stability of slides spotted with lipid/shRNA mixtures and with lipid/siRNA mixtures. We printed replica slides and compared both transfection efficiency and silencing efficiency at various time points. We did not observe any reduction in the performance of the shRNA arrays after 1 week, 1 month, or up to 2 months of storage at 4°C. In contrast, siRNA printed slides showed more variability, and unclear results were obtained after 2 weeks of storage.

An *in Situ* Assay for Defects in Proteosome Function. The need to locate transfected cells to score phenotypes on the array led to the consideration of phenotypic assays that depended on the expression of a fluorescent, exogenous reporter gene. The basic idea, a variation of the validation experiments described above, was to include in the transfection mix a plasmid harboring a fluorescent reporter that is differentially expressed (at higher or lower level) in cells in which RNAi has been used to alter the function of a specific pathway. To test this approach, we focused on protein half-life as a determinant of steady-state expression levels. A variety of motifs have been found to confer a short lifetime on cellular proteins. So-called PEST sequences are rich in the amino acids Pro (P), Asp, Glu (E), Ser (S), and Thr (T), which occur in internal positions in the sequence. Proteins containing PEST sequence elements are rapidly targeted to the 26S proteasome for degradation (12).

The mouse ornithine decarboxylase (MODC) has an extremely short half-life (13). MODC degradation is mediated by an internal domain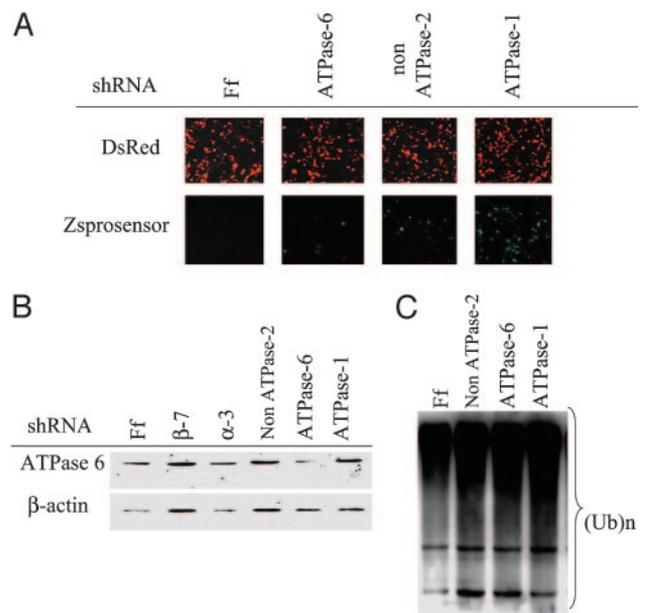, called MODC-d410, that contains several PEST motifs. This functional motif is transferable, decreasing greatly the stability of proteins to which it is fused (14, 15). This property has been exploited to create commercially available reporter systems in which MODC-d410, appended to a fluorescent protein, creates a fusion that can indicate the integrity of the proteosome in living cells.

We chose to analyze the expression level of a commercially available reporter consisting of a green fluorescent protein (ZsGreen) tagged on the carboxyl-terminus with the MODC-d410 domain (ZsProSensor, Clontech). We recently screened a library of 7,000 individual shRNAs for the ability to antagonize proteosome function in a 96-well plate format (28). Roughly one-quarter of primary positives targeted proteosome subunits. Putative positives from that screen were used on microarrays to validate the *in situ* approach and to compare the sensitivity of array-based assays to those carried out in 96-well plates. Based on these previous studies, thirty different hairpins targeting proteasome subunits were deposited, each in individual spots, together with the destabilized green reporter and a dsRed vector. As in previously described experiments, dsRed served as transfection control.

After 24 h of incubation we observed higher levels of ZsGreen protein in several dots containing proteasome shRNAs compared to control shRNAs, whereas no changes were observed in the intensity of the red fluorescent protein. During the following 48 h the green fluorescent signal gradually increased in these positive spots, achieving maximum intensity after 60–72 h. We identified clear differences in the accumulation level of the reporter in spots containing proteasome shRNAs compared with nonproteasome hairpins. Interestingly, the most intense signals were revealed from spots containing shRNAs that target subunits of the 19S base (Fig. 3*A*).

To confirm that the increased expression of the reporter was associated with alterations in proteasome function, we verified that cells transfected with a hairpin against the ATPase subunit 6 indeed showed a specific reduction of the targeted protein. As expected, Western blot analysis of transiently transfected 293T
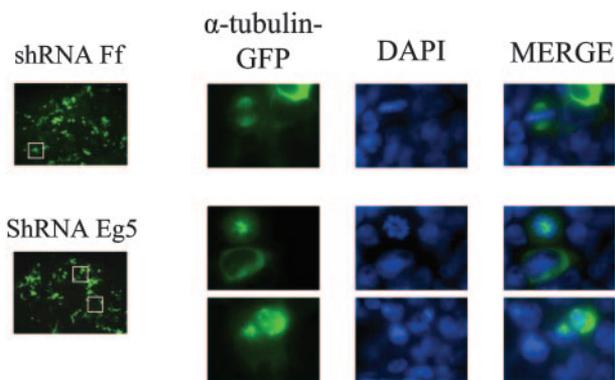
Fig. 4. Cytokinesis defects induced by Eg5 shRNAs. (*Upper*) Sample of normal mitotic metaphase detected in a dot containing firefly (control) shRNA. (*Lower*) Two typical "rosette" phenotype found in a printed spot containing the shRNA-7 against the motor protein Eg5.

cells with the ATPase-6 shRNA-1 showed a specific reduction in the level of the targeted protein (Fig. 3*B*).

It has been shown previously that in cells in which the normal function of the proteasome is blocked, there is an accumulation of polyubiquitinated proteins (16, 17). To validate further the antagonism of proteosome function by RNAi, we examined the level of polyubiquitinated proteins. Indeed, analysis of bulk ubiquitinated proteins by Western blotting with a ubiquitin antibody revealed an increase in these normally unstable species in cells treated with proteasome shRNAs compared with controls (Fig. 3*C*).

A Screen for Alterations in Cell Cycle Control: Cytokinesis Defects. The aforementioned screen was amenable to the use of microarray scanners to score positives by their ratio of fluorescent signals. To examine the suitability of this approach for other types of screens, we performed a live-cell microarray assay to identify cytokinesis defects induced by RNAi. As a reconstruction experiment, we knocked down the mitotic motor protein Eg5, because cytokinesis defects in cells where Eg5 function is inhibited are well established (18, 19).

The mitotic spindle, which consists of a dynamic array of microtubules and associated proteins, is responsible for segregation of chromosomes during mitosis. Studies using immunodepletion (20, 21) of the motor kinesin Eg5 or with the specific inhibitor monastrol (18) have revealed that inhibition of the normal function of this protein causes a defect in spindle formation. Initially, a defect in centrosome separation causes the assembly of monopolar spindles, and eventually, aberrant structures form that look like "rosettes" of microtubules with DNA at the periphery.

Based on the expectation of this typical morphology, we printed DNA–lipid complexes containing individual shRNAs targeting Eg5 on microarray slides. Transfection mixes also contained a plasmid encoding an α-tubulin GFP fusion protein. In this array, the GFP fusion protein identifies the cells that have been transfected and allows visualization of microtubules. Additionally, when the microarray was scored, Hoechst 33342 was added to the media to allow visualization of chromosomes. The analysis of the array revealed two hairpins that produced cells displaying the characteristic "rosette" pattern (Fig. 4). We did not observe this phenotype in any of the spots containing control shRNAs. This phenotype was also observed when shRNAs targeting Eg5 were tested in a 96-well plate format and was similar to the phenotype obtained after Eg5 inhibition by monastrol (data not shown).

The use of vectors harboring reporters or fusion proteins is a very convenient approach to identify abnormal phenotypes by *in situ*

transfection. However, appropriate reagents will not be easily available for all interesting phenotypes. For this reason, we asked whether it was possible to identify Eg5 suppression phenotypes by the conventional technique of immunofluorescence (IF). A replica of the Eg5 glass slide, in which the α-tubulin fluorescence reporter was replaced by dsRed, was stained with a standard IF protocol. We find that we could easily identify cytokinesis defects produced by the same shRNAs identified with the α-tubulin GFP protein by using this methodology (data not shown).

Discussion

Genomewide analyses of loss-of-function phenotypes in mammals, similar to classic genetic studies in yeast, were very difficult, if not impossible, only a few years ago. However, over the last several years RNAi has emerged as a powerful approach for manipulating gene expression in mammalian cells, opening the door to the execution of such screens. High-throughput RNAi analyses have previously been used to study gene function in *D. melanogaster* and *C. elegans*. For example, essential genes (22), G protein-coupled receptors (GPCRs) (23), fat regulatory genes (24), and genes that regulate lifespan (25) have been functionally analyzed by this approach. Unfortunately, similar studies in mammals still represent a technological challenge. In part, limitations occur because of the cost of the RNA species themselves and the cost of introducing these species (siRNA and shRNA) into mammalian cells. Additionally, the use of a large-scale analysis in any system is limited by the screening methodology.

Here we validate the use of a cost-effective high-throughput procedure for RNAi-based screens in mammalian cells. This procedure is based on methodologies developed by Sabatini and colleagues (11) for creating high copy suppression phenotypes by "reverse transfection." This allows for the cost-effective use of materials, both the nucleic acids themselves and tissue culture reagents. We estimate that between 100 and 500 reverse transfections can be done with the materials required for a single transfection in a well of a 96-well plate. Additionally, thousands of samples can be printed in parallel on a glass-slide microarray, reducing the time and cost associated with maintaining cultures and analyzing phenotypic outputs. Finally, as previously described, printed slides can be stored for several months without losing potency (11).

By comparing results obtained by initiating RNAi *in situ* on microarrays to screens conducted in 96-well plates, we find that the arrays compare favorably to standard methods for both sensitivity and specificity. In agreement with our data, two recent papers have reported that RNAi could be initiated on printed slides to inhibit the expression of a co-delivered marker gene (26, 27). Our study extends these results by showing that a similar procedure can be used to silence endogenous genes to create RNAi-induced phenotypes relevant to two independent biological pathways.

Firstly, we designed an assay to study proteosome-mediated degradation. As predicted, when subunits of the 26S proteasome were targeted by shRNAs, we could clearly identify accumulation of an engineered protein that is normally degraded by the proteasome pathway. We showed that proteolytic defects were due to specific suppression of the targeted 26S subunits and demonstrated that cellular levels of the natural proteasome substrates (ubiquitinated proteins) were affected in the same way as the fluorescent reporter. In a second study, we analyzed the effect produced by loss of kinesin Eg5 as model for cytokinesis defects. After targeting with Eg5 shRNAs, we could reproduce the expected aberrant spindle morphology in a printed slide format, while no changes were observed in control spots.

Here, we demonstrate the feasibility of using printed arrays of siRNAs and shRNAs for highly parallel phenotype analysis in living cells. This approach is flexible and provides low-cost alternatives to similar screens carried out in multiwell plate formats. As large libraries of shRNAs become widely available

GENETICS

(28, 29), the techniques described herein will become a powerful approach to genetic analysis in mammalian cells.

1. Zamore, P. D. (2001) *Nat. Struct. Biol.* **8,** 746–750.
2. Hannon, G. (2002) *Nature* **418,** 244–251.
3. Maeda, I., Kohara, Y., Yamamoto, M. & Sugimoto, A. (2001) *Curr. Biol.* **11,** 171–176.
4. Ashrafi, K., Chang, F. Y., Watts, J. L., Fraser, A. G., Kamath, R. S., Ahringer, J. & Ruvkun, G. (2003) *Nature* **421,** 268–272.
5. Pothof, J., van Haaften, G., Thijssen, K., Kamath, R. S., Fraser, A. G., Ahringer, J., Plasterk, R. H. & Tijsterman, M. (2003) *Genes Dev.* **17,** 443–448.
6. Somma, M. P., Fasulo, B., Cenci, G., Cundari, E. & Gatti, M. (2002) *Mol. Biol. Cell.* **13,** 2448–2460.
7. Kiger, A., Baum, B., Jones, S., Jones, M., Coulson, A., Echeverri, C. & Perrimon, N. (2003) *J. Biol.* **2,** 27.
8. Tabara, H., Grishok, A. M. &. Mello. C. C. (1998) *Science* **282,** 430–431.
9. Timmons, L. & Fire, A. (1998) *Nature* **395,** 854.
10. Clemens, J. C., Worby, C. A., Simonson-Leff, N., Muda, M., Maehama, T., Hemmings, B. A. & Dixon, J. E. (2000) *Proc. Natl. Acad. Sci. USA* **97,** 6499–6503.
11. Ziauddin, J. & Sabatini, D. M. (2001) *Nature* **411,** 107–110.
12. Rechsteiner, M. & Rogers, S. W. (1996) *Trends Biochem. Sci.* **21,** 267–271.
13. Murakami, Y., Matsufuji, S., Kameji, T., Hayashi, S., Igarashi, K., Tamura, T., Tanaka, K. & Ichihara, A. (1992) *Nature* **360,** 97–99.
14. Olmo, M. T., Rodriguez-Agudo, D., Medina, M. A. & Sanchez-Jimenez, F. (1999) *Biochem. Biophys. Res. Commun.* **257,** 269–272.
15. Verma, R. & Deshaies, R. J. (2000) *Cell* **101,** 341–344.
16. Wojcik, C. & DeMartino, G. N. (2002) *J. Biol. Chem.* **277,** 6188–6197.
17. Bochtler, M., Ditzel, L., Groll, M., Hartmann, C. & Huber, R. (1999) *Annu. Rev. Biophys. Biomol. Struct.* **28,** 295–317.
18. Mayer, T. U., Kapoor, T. M., Haggarty, S. J., King, R. W., Schreiber, S. L. & Mitchison, T. J. (1999) *Science* **286,** 971–974.
19. Goshima, G. & Vale, R. D. (2003) *Cell Biol.* **162,** 1003–1016.
20. Sawin, K. E., LeGuellec, K., Philippe, M. & Mitchison, T. J. (1992) *Nature* **359,** 540–543.
21. Blangy, A., Lane, H. A., d'Herin, P., Harper, M., Kress, M. & Nigg, E. A. (1995) *Cell* **83,** 1159–1169.
22. Maeda, I., Kohara, Y., Yamamoto, M. & Sugimoto, A. (2001) *Curr. Biol.* **11,** 171–176.
23. Keating, C. D., Kriek, N., Daniels, M., Ashcroft, N. R., Hopper, N. A., Siney, E. J., Holden-Dye, L. & Burke, J. F. (2003) *Curr. Biol.* **13,** 1715–1720.
24. Ashrafi, K., Chang, F. Y., Watts, J. L., Fraser, A. G., Kamath, R. S., Ahringer, J. & Ruvkun, G. (2003) *Nature* **421,** 268–272.
25. Lee, S. S., Lee, R. Y., Fraser, A. G., Kamath, R. S., Ahringer, J. & Ruvkun, G. (2003) *Nat. Genet.* **33,** 40–48.
26. Mousses, S., Caplen. N. J., Cornelison, R., Weaver, D., Basik, M., Hautaniemi, S., Elkahloun, A. G., Lotufo, R. A., Choudary, A., Dougherty, E. R., *et al.* (2003) *Genome Res.* **13,** 2341–2347.
27. Kumar, R., Conklin, D. S. & Mittal, V. (2003) *Genome Res.* **13,** 2333–2340.
28. Paddison, P. J., Silva, J. M., Conklin, D. S., Schlabach, M., Li, M., Aruleba, S. Balija, V., O'Shaughnessy, A., Gnoj, L., Scobie, K., *et al.* (2004) *Nature* **428,** 427–431.
29. Berns, K., Hijmans, E. M., Mullenders, J., Brummelkamp, T. R., Velds, A., Heimerikx, M., Kerkhoven, R. M., Madiredjo, M., Nijkamp, W., Weigelt, B., *et al.* (2004) *Nature* **428,** 431–437.

Silva *et al.*